Electronic Supplementary Material (ESI) for Journal of Materials Chemistry C.

Supporting Information

The Fabrication of Self-Powered $CuInS_2/TiO_2$ Heterojunction Photodetector and the Application in Visible Light Communication with Ultraviolet Light Encryption

Menghan Li, Jianping Xu, Kuifeng Zhu,* Shaobo Shi, Qiuyang Zhang, Yichen Bu, Jing Chen, Jianghua Xu, Qin Zheng, Yanjie Su, Xiaosong Zhang, and Lan Li**

School of Science, Tianjin University of Technology, Tianjin 300384, China.

Tianjin FLY Technology Company Limited, Tianjin 300385, China

School of Science, Key Laboratory of Display Materials and Photoelectric Devices, Ministry of Education and Tianjin Key Laboratory for Photoelectric Materials and Devices, Tianjin University of Technology, Tianjin 300384, China.

School of Science, Tianjin University of Technology and Education, Tianjin 300222, China

*E-mail: xjp0335@163.com (Jianping Xu)

*E-mail:18622029890@126.com (Kuifeng Zhu)

*E-mail:lilan2000us@126.com (Lan Li)

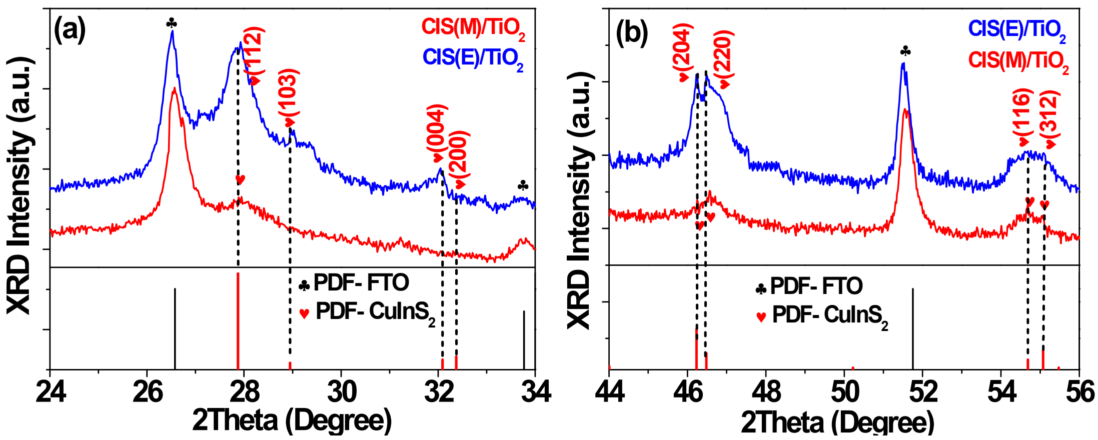

Fig.S1 Enlarged view of CIS XRD patterns for (a) (112), (103), (004) and (200) crystal planes, and (b) (204), (220), (116) and (312) crystal planes

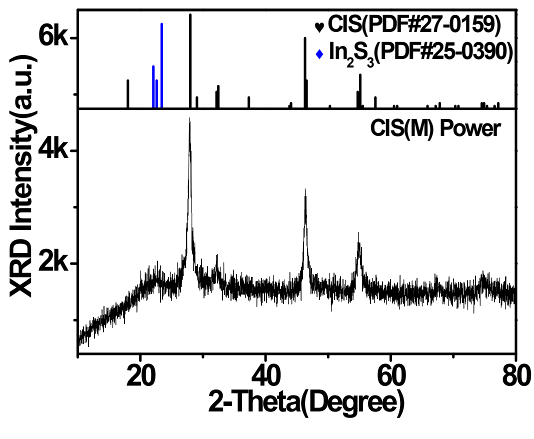

Fig.S2 XRD pattern of CIS powder grown in mixed solvent

Fig.S2 shows the XRD pattern of CIS powder grown in mixed solvent. Except for the weak diffraction peak of In_2S_3 at $2\theta=22.5°$(PDF#25-0390), all other peaks are single chalcopyrite CIS(PDF#27-0159). The solubility product k_{sp} of In_2S_3 is 5.7×10^{-74} and the solubility product k_{sp} of Cu_2S is 3×10^{-48}. Because the solubility product of In_2S_3 is smaller than Cu_2S, and the In^{3+}concentration in the reaction precursor solution is larger than Cu^+, the growth rate of In^{3+} in the early stage of reaction is larger than Cu^+, which results in the proportion of In being greater than Cu during the growth process, and In_2S_3 impurities are more likely to be generated.

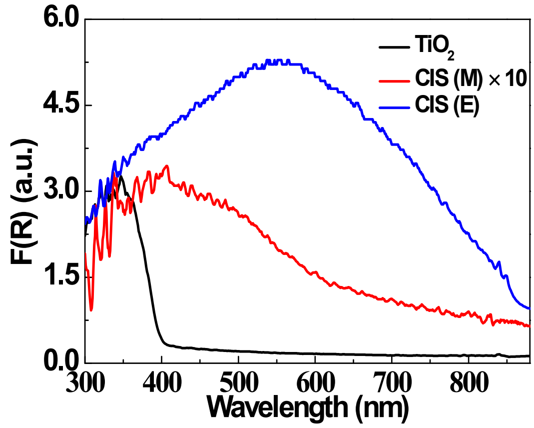

Fig.S3 F(R) spectra in incident light with different wavelengths

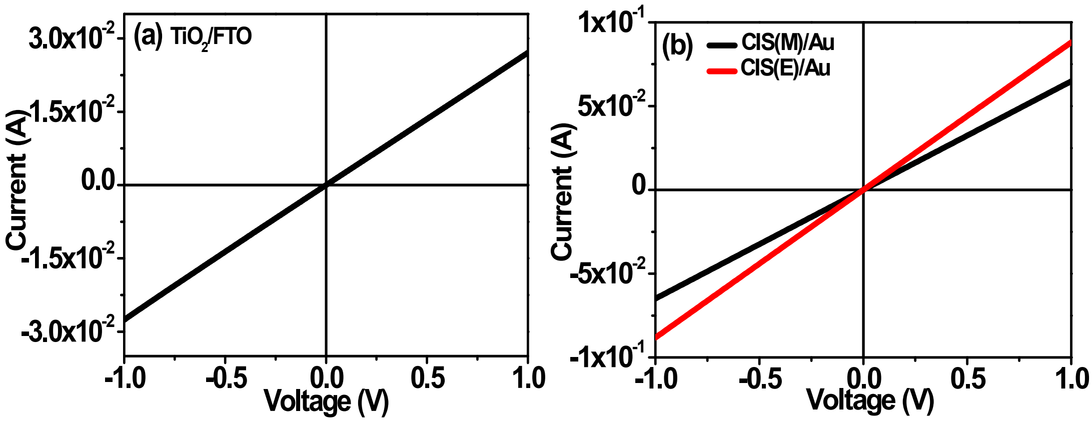

Fig.S4 I-V curves of (a) FTO/TiO_2 and (b) CIS/Au

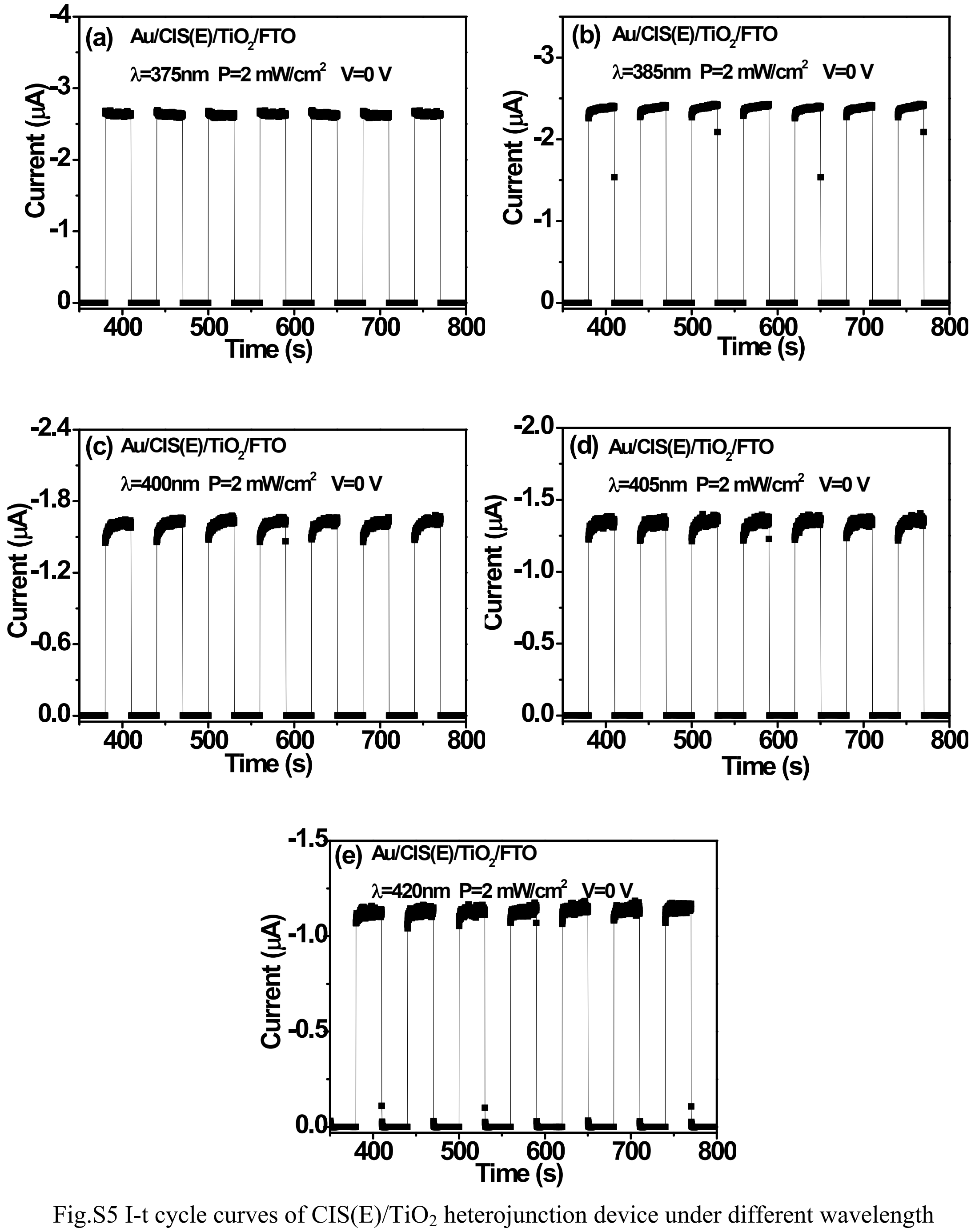

Fig.S5 I-t cycle curves of CIS(E)/TiO_2 heterojunction device under different wavelength illumination

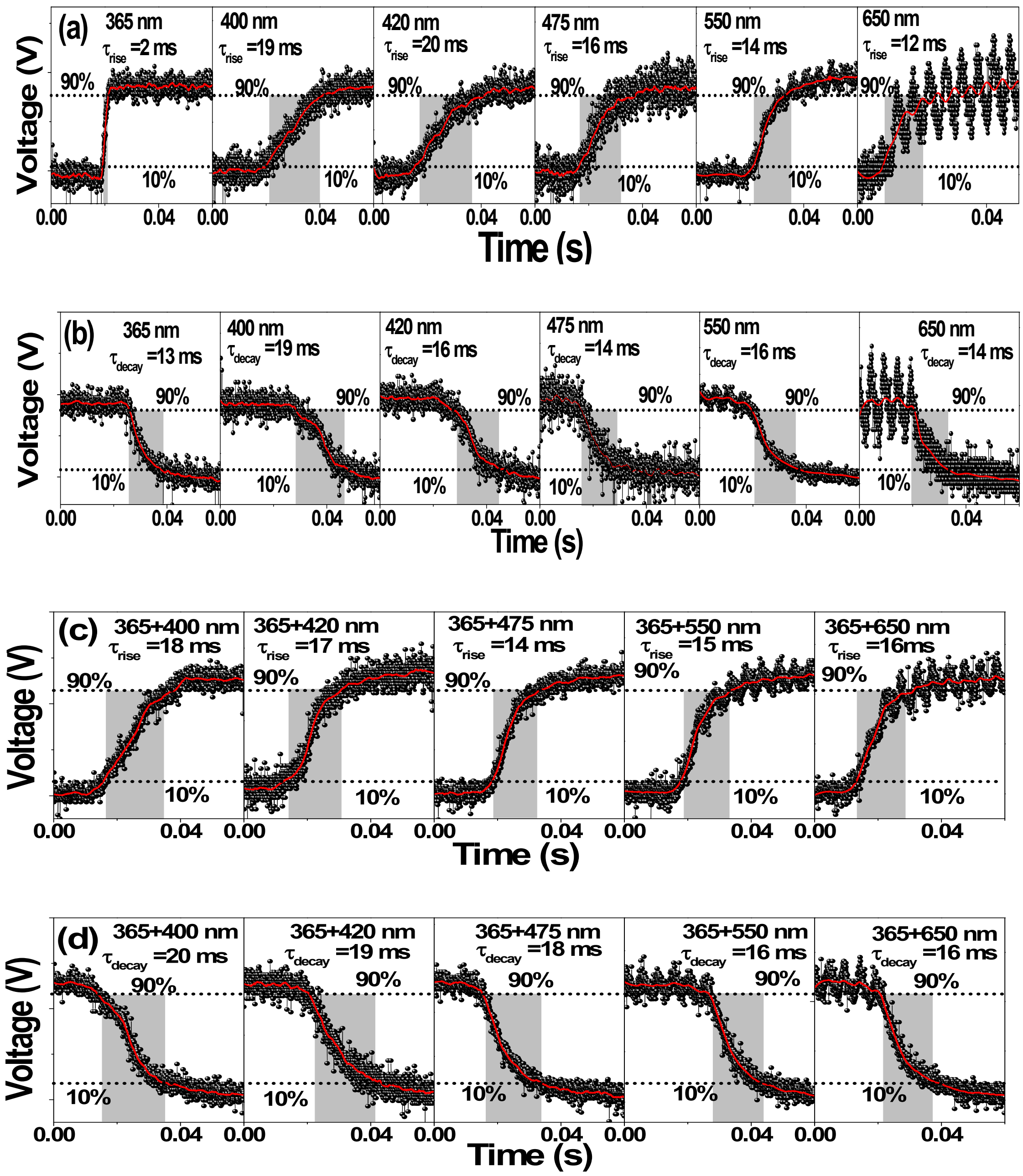

Fig.S6 (a) Response time and (b) Decay time of CIS(E)/TiO_2 heterojunction PD under monochromatic light irradiation. (c) Response time and (d) Decay time under simultaneous irradiation of UV (365 nm) and visible light with different wavelengths

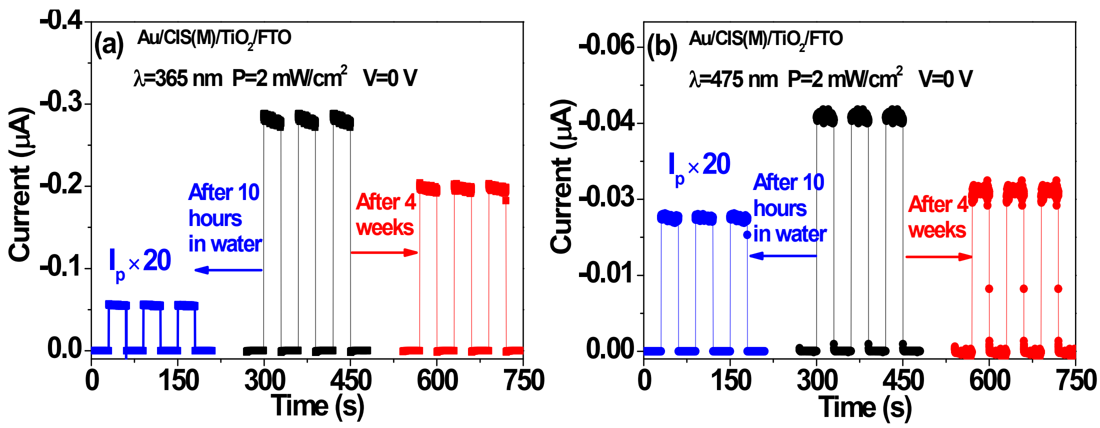

Fig.S7 The poor stability of CIS(M)/TiO_2 heterojunction PD under (a) 365 nm and (b) 475 nm light illumination

Table S1. Cu/In ratio of the CIS films at surface and bulk

Samples	Cu/In Ratio Surface (XPS)	Cu/In Ratio Bulk (EDS)
CIS(M)/TiO_2	0.44	0.72
CIS(E)/TiO_2	0.83	0.98

Table S2. Information about TiO_2 NRs and CIS films obtained from XPS and M-S spectra

Samples	N_D (cm^{-3})	N_A (cm^{-3})	V_{FB} (V)	VB (eV)
TiO_2	4.67×10^{19}	--	-0.69	2.62
CIS(M)	--	8.23×10^{19}	0.03	0.93
CIS(E)	--	6.01×10^{20}	-0.25	0.68

Photodetector	Wavelength (nm)	Bias (V)	D* (Jones)	R (mA/W)	I_{ph}/I_d	T_r (ms)	Ref.
Organics/CIS-ZnS Core-Shell QDs/Organics	450	-40 (V_{GS})	3.76×10^{11}	860	120	< 5	16
SiO_2/CIS-ZnS Core-Shell QDs - graphene/Au	660 (5 mW)	V_{DS}	--	35×10^{3}	--	--	19
ITO/ZnO-CIS QDs/TFB/PEDOT:PSS/Al	620 (14.2 mW/cm^2)	0	2.5×10^{10}	0.53	--	--	20
Si/SiO_2/MoS_2/CIS QDs/AuNPs	635	4.5 (V_{DS})	2.27×10^{12}	16.65×10^{3}	24.1	5×10^{2}	21
ITO/TiO_2/PV							

K:CIS-ZnS QDs/MoO_3/Ag							
Si/SiO_2/CIS-ZnS QDs/UCNP	980	25	--	--	--	--	23
FTO/TiO_2/CIS /Au	365 (2 mW/cm^2)	0	1.3×10^{12}	44.8	2.7×10^{4}	2	This work
FTO/TiO_2/CIS /Au	650 (2 mW/cm^2)	0	4.7×10^{11}	15.6	9.2×10^{3}	12	This work

Table S3. Performance parameters based on CIS PDs